TWSME of a NiTi strip in free bending conditions: experimental and theoretical approach

A. Fortini, M. Merlin, R. Rizzoni
Department of Engineering (EnDiF), University of Ferrara, (Italy)
annalisa.fortini@unife.it, mattia.merlin@unife.it, raffaella.rizzoni@unife.it

S. Marfia
Department of Civil and Mechanical Engineering (DiCeM), University of Cassino and Lazio Meridionale, (Italy)
marfia@unicas.it

ABSTRACT. This paper deals with the two-way shape memory effect (TWSME) induced on a strip of a near-equiatomic NiTi alloy by means of the shape memory cycling training method. This procedure is based on the deformation in martensite state to reach the desired cold shape followed by cycling the temperature from above A_f to below M_f. To this end, the sample was thermally treated to memorise a bent shape, thermomechanical trained as described and thermally cycled in unloaded conditions in order to study the stability of the induced TWSME. Heating to A_f was reached by a hot air stream flow whereas cooling to M_f was achieved through natural convection. The evolution of the curvature with the increasing number of cycles was evaluated. The thermomechanical behaviour of the strip undergoing uniform bending was simulated using a one-dimensional phenomenological model based on stress and the temperature as external control variables. Both martensite and austenite volume fractions were chosen as internal parameters and kinetic laws were used in order to describe their evolution during phase transformations. The experimental findings are compared with the model simulation and a numerical prediction based on the approach proposed in [25].

KEYWORDS. NiTi-based alloys; two-way shape memory effect; thermomechanical training; bending.

INTRODUCTION

Shape memory alloys (SMAs) are an interesting class of metallic materials with the ability of recovering seemingly permanent deformation when they are deformed in the martensitic low temperature phase and subsequently heated to the austenitic high temperature phase. Shape memory effect (SME) and superelasticity (SE) are associated with diffusionless solid-state transformations between two crystallographic phases: the cubic crystal structure, stable at high temperature, and the monoclinic crystal structure, stable at low temperature. The forward transformation from austenite to martensite occurs during cooling, begins at the martensitic start temperature M_s and ends at the martensitic finish temperature M_f. The reverse transformation from martensite to austenite occurs upon heating, begins at the austenitic start temperature A_s and finishes at the austenitic finish temperature A_f.
Over the last decades a wide variety of SMAs have been investigated and several compositions have been studied, by adding different alloying elements (such as zinc, copper, gold and iron) to existing alloys. Among the different shape memory alloys compositions, the NiTi alloy system is the most extensively studied and used in the greatest number of commercial applications mainly because of its excellent mechanical properties, high corrosion resistance and

biocompatibility. In particular, the near-equiatomic NiTi alloys are the most important practical shape memory alloys, extensively used for an increasing number of applications in different fields of engineering.
The NiTi alloy system, in addition to the one-way shape memory effect (OWSME) may also show the two-way shape memory effect (TWSME). Through the SME the material could recover the macroscopic shape of the austenitic parent phase upon heating above A_f, while through the TWSME, it also exhibits a return to the reoriented martensitic shape upon cooling below M_f, in the absence of applied stress. This spontaneous repeatable shape change on heating and cooling is an acquired behaviour, rather than an inherent property of the material, obtained by specific thermomechanical loading cycles, named training treatments, to which the SMA has been subjected [1, 2]. This procedure develops a residual internal stress state which guides the growth of certain martensitic variants, towards the preferred orientations, regarding the deformation adopted during training, when SMA is stress-free cooled [3]. From a crystallographic point of view, it is widely accepted that preferential martensite formation is due to the generation of permanent defects in the parent phase resulting from training procedure [2, 4]. As a result the material will change its shape as it changes its phase. Different training methods for obtaining a TWSME are described in literature and the influence of the type and training parameters, the stability of the TWSME during thermal cycling as well as the efficiency of the methods have been widely investigated [1, 2, 5-10]. Generally, training procedures have the purpose to induce the low temperature shape in the sample introducing permanent defects such as dislocations, stabilised stress induced martensite and precipitates [4, 5, 11, 12]. Common methods of training include: shape memory cycling, pseudoelastic cycling, combined shape memory cycling/pseudoelastic cycling and constrained cycling of deformed martensite [1, 5, 13, 14]. All of these thermomechanical treatments deal with the repetition of a procedure that considers the transformation from austenite to a preferentially oriented martensite or from deformed martensite to austenite [13].
Due to their attractive behaviour, NiTi shape memory alloys have been successfully applied in a broad set of innovative applications in aerospace, biomedical, mechanical and civil engineering fields. In particular, SMAs are excellent materials to be used as actuating elements in smart structures given that they could generate large force and displacement during the phase transformation. Many active deformable structures, in which NiTi strips or wires are embedded in a polymeric matrix, are based on the OWSME and, as a consequence, an external force is required to bring back the structure to its original shape. To this end, the application of the TWSME on the SMA elements plays an important role since it make possible to achieve more compact and simple configuration systems with improved performances upon demand, thanks to the integration of multiple functions in a single component. A TWSME behaviour in bending gives the macroscopic reversible shape change of the functional structure upon heating and cooling, without demanding the recovery to the elasticity of the polymeric structure.
The SME behaviour in bending has been experimentally and theoretically investigated by many authors. The works [15, 16] have focused on the bending properties of polymer-SMA composite microdevices, for example, microvalves. In these actuators, the right combination of the polymer and SMA thin film leads to a two-way stable behaviour during heating and cooling. More recently, Roh and Bae [17] have numerically and experimentally investigated the thermo-mechanical behaviour of NiTi strips associated with stress and temperature-induced transformations. The activation of the SMA strips causes a bending deformation on the actuator, which has remarkable vertical tip deflections. Larger deflections can be obtained by increasing the initial strain of the SMA. Irzhak et al. [18] observed giant reversible bending deformation at a sub-micrometre scale by using a nichel-SMA composite strip. Furthermore, some authors focused on the effects of the pre-strain, recovery temperature and bending deformation on the shape memory effects [9, 19-24]. To predict the one-dimensional thermomechanical behaviour of SMA, several macroscopic constitutive models are currently available in literature, an overview can be found in [3, 23, 25-28]. It is widely known that the response of SMA is dependent on stress and temperature fields and it is closely connected with the crystallographic phase of the material and the thermodynamics underlying the transformation processes.
While some studies are focused on the two-way shape memory effect exhibited by bent wires [9, 13, 19], the present study is aimed at investigating the stability of the TWSME behaviour induced on near-equiatomic NiTi strips by means of the so-called shape memory cycling method, which here is applied to bending deformations. In particular, the possibility to take advantage of the TWSME is here considered in order to optimise the behaviour of strips embedded in active deformable structures. To this end, a strip is firstly subjected to a specific thermomechanical treatment, in order to memorise a bent shape with a uniform curvature, and then trained to realise the spontaneous recovery to the martensitic shape upon cooling. In particular, the training process basically consists of the repetition of the following steps: i) cooling the SMA to below M_f to form martensite, ii) deforming to the desired cold shape, below the shape memory limit, iii) heating in stress-free condition to above A_f to recover the original high temperature shape [13, 14]. It should be highlighted that the amount of spontaneous shape change on cooling is significantly less than those being induced in the ii) deformation step and it is typically between 0.2 and 0.25% of the training strain value [4, 14]. After the training

procedure, the stability of the induced TWSME with the increasing number of cycles is assessed considering the curvatures assumed at each cycle on heating/cooling. Moreover, the behaviour of the SMA undergoing bending is simulated by means of a phenomenological model, based on the use of stress and temperature as control variables, but proposing an original approximated relation for the evolution of the curvature with the temperature, according to the model developed in [20]. This relation, useful to practitioners, is coupled with a phenomenological description of the phenomena occurring during the training process, which are supposed to be based on the martensite accumulation during cycling. Shape recovery simulations for the NiTi strip undergoing uniform bending are considered and the ability of the model to reproduce experimental data is evaluated. The resulting evolution of the curvature with the number of cycles obtained with this model is also compared with the experimental data. Furthermore, all these results are compared with a numerical simulation based on the model proposed in [25].

MATERIAL CHARACTERISATION

A commercial NiTi shape memory alloy of nominal composition Ni-50.8 at%Ti was used in the present study. A strip of 0.8 x 7 x 107 mm in dimension was cut by means of electro-erosion starting from a plane foil of the as-supplied material. In order to fix the strip during both the training process and the TWSME cycles, a "L" shape was chosen, as depicted in Fig. 1.

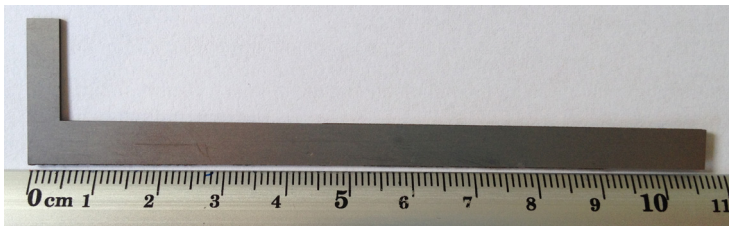

Figure 1: Strip shape.

The sample was annealed at 700 °C for 20 min followed by controlled cooling to room temperature, at a cooling rate of 1 °C/min, in order to delete any residual stresses of previous deformation history.
To evaluate the characteristic martensitic and austenitic starting and finishing temperatures as well as the latent heats per unit mass, a differential scanning calorimetry (DSC) test was carried out, after annealing, at a heating/cooling rate of 10 °C/min. The transformation temperatures (TTRs), summarised in Tab. 1, were extrapolated from DSC data through the tangential line method.

A_s [°C]	A_f [°C]	ΔH_A [MPa/°C]	M_s [°C]	M_f [°C]	ΔH_M [MPa/°C]
82	104	24.7	69	46	25.3

Table 1: Transformation temperatures and latent heats per unit mass obtained by DSC.

Mechanical properties of the material were obtained through uniaxial tensile tests performed at 25 °C and 150 °C respectively under displacement controlled loading conditions. An Instron 4467 testing machine with a 30 kN load cell was used and the loading rate of 1 mm/min was set in order to minimise the self-heating effect due to the transformation latent heat. According to TTRs data, the elastic modulus of the martensite, E_M, the transformation stresses at the onset/end of the martensitic plateau, σ_S and σ_F, and the maximum recoverable strain ε_L were estimated at 25 °C while the elastic modulus of the austenite, E_A, was estimated at 150 °C. These material properties are listed in Tab. 2.

σ_S [MPa]	σ_F [MPa]	ε_L	E_M [MPa]	E_A [MPa]	C_A [MPa/°C]	C_M [MPa/°C]
149	210	0.06	28423	63475	7.25	8.22

Table 2: Material properties obtained by tensile tests.

The stress-influence coefficients C_A and C_M were obtained using the Clausius-Clapeyron equation:

$$C_A = \frac{\rho \cdot \Delta H_A}{T_{CR} \cdot \varepsilon_L} \quad (1)$$

$$C_M = \frac{\rho \cdot \Delta H_M}{T_{CR} \cdot \varepsilon_L} \quad (2)$$

where the NiTi density ρ is assumed 6.45 g/cm^3 and the critical temperature T_{CR} is calculated as $(A_s+A_f)/2$.
To memorise the bent shape, the strip was subjected to a double heat treatment: it was previously strained at room temperature and wounded on a cylindrical jig to reach a circle shape. This fixture was placed into a tube furnace, heated at 450 °C for 25 min and quenched by water-cooling. These specific temperature and time were chosen according to the results of a previous experimental study [15], which demonstrated that this combination allows reaching a 92% of shape recovery. Subsequently, the strip was strained at room temperature applying opposite bending couples acting at the ends and locked into an arc clamp. The strip was thus thermally treated as previous to memorise this bent shape, with an initial curvature radius R_0 equal to 42.32 mm.

Training procedure

The heat-treated NiTi strip was subjected to the thermomechanical cycling by means of the shape memory cycling method [13]. A specifically designed training sequence was applied to the sample repeating the following steps for 30 cycles: pre-straining at a T< M_f (room temperature) to reach the desired cold shape, ii) heating the specimen above A_f (140 °C) through a hot air stream flow, iii) cooling below M_f (room temperature) by natural convection.
Therefore, the strip was strained to a flat shape, applying a uniform bending load at room temperature, and fixed into a supporting structure, with one end held in a clamp. In order to ensure reaching the phase transformation temperature on heating, a K-type thermocouple was placed in the inner radius of the strip and kept in good thermal contact with it by conductive aluminum tape. Heating the strip to high temperature above A_f was achieved by hot air stream flow whereas cooling to room temperature, below M_f, was realised through natural convection. To study the curvature evolution, sample images were acquired by a digital camera at the end of the heating process, Fig. 2a, as well as after cooling to room temperature, Fig. 2b. Interpolating the axis of the strip with a three-point arc, by means of a CAD software, the hot radius, R_H, and the cold radius, R_C, were collected.

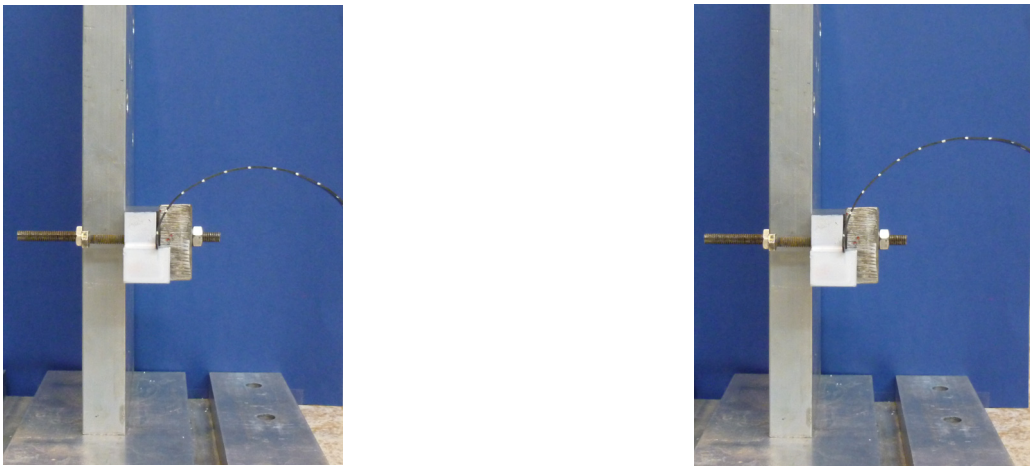

(a) (b)

Figure 2: (a) Hot shape; (b) Cold shape.

It is well known that there is a limit to the amount of reversible strain that can be achieved in TWSME [14]. In particular, the two-way recoverable strain is significantly less than the one-way recoverable strain and it is typically in the neighborhood of 2%. In the present study the bending deformation strain was calculated according to Eq. (3):

$$\varepsilon_{tr} = \frac{t}{t + 2R_0} \quad (3)$$

where t is the thickness of the strip and R_0 is the radius of the memorised shape. Therefore, the target two-way recoverable strain between the desired hot shape of the arc and the desired cold shape of the straight line, in this case was equal to 0.9%, less than the threshold of 2%.
The amount of TWSME was assessed by thermally cycling the trained strip without any applied external stress. To evaluate the stability of the two-way memory behaviour, 30 cycles were performed.

RESULTS AND DISCUSSION

Experimental results

The evolution of hot and cold shapes over the range of the training cycles is reported in Fig. 3a. The desired hot shape corresponds to the curvature = $1/R_0$= 23.63 * 10^{-3} mm^{-1} of the memorised arc, while the desired cold shape corresponds to the straight line and it is therefore equal to 0. During the training process, the evolution of hot curvature suggests that, apart from the initial cycles where a gradual loss in the memorised shape occurs, the data level off to a value close to 15 * 10^{-3} mm^{-1}. As regard the cold curvature, the curve trend decreases as the numbers of training cycles increases. As can be seen, the difference between hot curvature and cold curvature progressively increases and reaches the maximum value of 7.26 * 10^{-3} mm^{-1} after 30 cycles. It is known that the training process is aimed at producing dislocation arrangements that create an isotropic stress field in the austenite phase, responsible for the further spontaneous shape change upon cooling. However, the dislocation structure is often accompanied by a permanent strain that would degrade the memory of the hot shape [13]. According to the results reported in Fig. 3a it is clear that the deformation in full martensitic state and the consequent progress of dislocation arrangements are linked to the loss of memory for the hot shape with increasing the number of training cycles. As regards the cold curvature and its progressively decrease to the desired cold shape it is likely that in the initial cycles the dislocation arrangements are readily introduced and, due to the greatly increase, the level of memory in the cold shape runs up [13]. As a result, at each cycle the amount of single-variant martensite increases, improving the memory of the cold shape.
The amount of two-way behaviour through training cycles is calculated as the difference and depicted in Fig. 3b. is the curvature at the austenite state (hot) and is the curvature at the martensite (cold) state. The gradual increase with training cycles is consistent with the progressive stabilisation of the behaviour achieved by the training procedure. It should be highlighted that, as depicted in Fig. 3a, the increase of the two-way behaviour reported in Fig. 3b is completely due to the improved cold curvature behaviour, which gets closer to the desired cold shape, rather than the hot curvature evolution, which is almost steady as the number of cycles increases.
The spontaneous shape change, simply upon heating and cooling, was assessed through additional 30 cycles (TWSME cycles). The curvature values assumed by the strip at each cycle are reported in Fig. 4 from which it is evident that, while the hot curvature has a slightly increase to the desired hot shape, the cold curvature shows a quite constant evolution rather than a decrease to the desired cold shape. The difference between the hot and cold curvature is almost constant with increasing the number of cycles, but this doesn't mean the establishment of the two-way behaviour. It can be pointed out that during the TWSME cycles, where no external stress is applied, the amount of single-variant martensite will decrease and, as a result, the cold behaviour moves away from the desired cold shape.

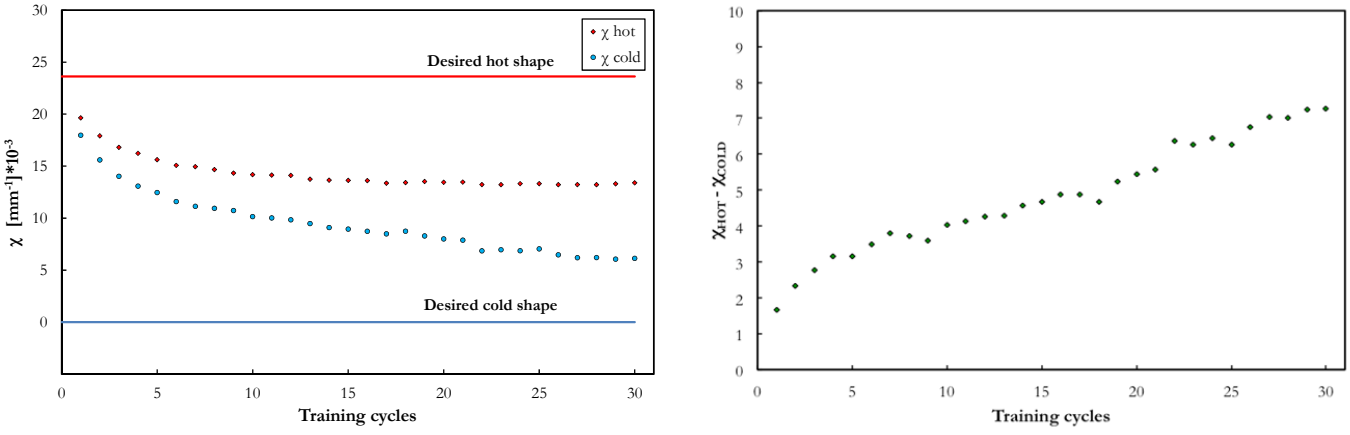

(a) (b)

Figure 3: (a) Comparison of hot and cold curvature curves versus training cycles; (b) Two-way behaviour versus training cycles.

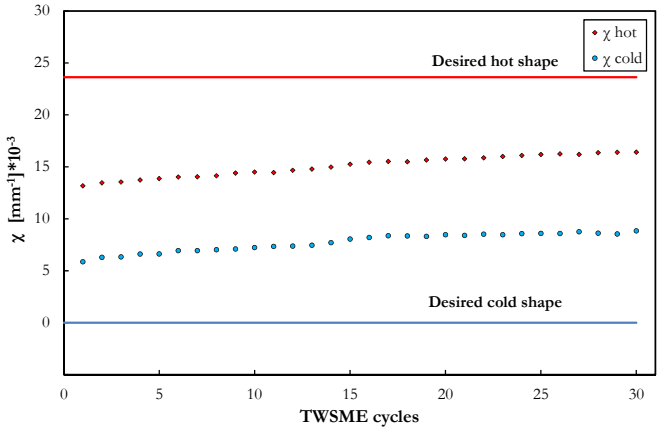

Figure 4: Two-way recoverable shape change versus TWSME cycles.

CONSTITUTIVE MODELLING

The thermomechanical behaviour of the SMA strip in bending is simulated by using the results obtained in [20], which are briefly reviewed in this section. In [20] a one-dimensional phenomenological model is adopted, based on external control variables, the stress σ and the temperature T, and on internal variables, which are the single-variant martensite, multi-variant martensite and austenite volume fractions.

The phase production processes that are considered during bending and free shape recovery under heating are the following: during bending at low temperature, multi-variant martensite transforms into single-variant martensite; during shape recovery upon heating, both multi-variant and single-variant martensite volume fractions transform to austenite. Each phase production is detailed by kinetic equations describing the evolution of the phase fractions during transformation in terms of the current values of the stress and the temperature. The kinetic equations are assumed to be linear for simplicity and the reader is referred to [20] for further details.

The stress σ is related to the strain ϵ via the following constitutive Eq. (4):

$$\sigma = \begin{cases} E\left(\epsilon - \epsilon_L \xi_s\right) & \text{if } \epsilon \geq 0 \\ E\left(\epsilon + \epsilon_L \xi_s\right) & \text{otherwise} \end{cases} \tag{4}$$

Here ϵ_L>0 is the maximum strain achievable by the transformation of multi-variant into single-variant (detwinning), E is the elastic modulus, assumed to take the same value, 28423 MPa, for all the three phases and ξ_s is the single-variant martensite volume fraction. The behavior is assumed symmetric in traction and compression.

The first bending at low temperature ($T<M_f$) of the NiTi strip is modeled as the uniform bending of a beam entirely made of multi-variant martensite. The beam is taken to be l =107 mm long, and it has the same rectangular cross-section of the NiTi strip, with thickness h = 0.8 mm and width b = 7 mm. Two opposite couples are applied to the ends of the beam, to bend it from the initial memorised curvature χ_0 = 23.63 * 10^{-3} mm^{-1} to the final curvature reached after elastic springback χ_r= 0.00 m^{-1}, corresponding to a flat shape.

Using the Euler-Bernoulli theory as done in [20], it can be shown that during bending single-variant forms initially at the outer and inner fibers of the cross-section and the transformation spreads inside the beam as the value of the applied couples is further increased. The residual stress and single-variant martensite distributions, calculated using the material data listed in Tab. 2, are piecewise linear and they are shown in Fig. 5. In the following, λ will denote the distance from the neutral axis to the level at which the residual single-variant fraction ξ_{sr} vanishes.

For the free shape recovery under heating, a semi-analytical solution is proposed in [20] and here applied for the data of the alloy studied in this paper. The solution, valid under the assumption of a uniform temperature distribution throughout the cross-section, is based on the existence of transformation fronts, nucleating from the points where the residual stress vanishes and evolving with the temperature. Indeed, the kinetic relations for the transformation of multi and single-variant martensite into austenite considered in [20] impose that points at zero stress transform first. There are two points at which the residual stress vanishes: one is the origin, and the other is calculated at the distance $z_0(A_s)$ = 0.27 mm from the origin. The single-variant martensite is absent at the origin (cfr. Fig. 5), thus from the origin only a front nucleates, that one for

the transformation of the residual multi-variant martensite into austenite. This front is denoted z_m in Fig. 6. From the point $z_0(A_s)$ two transformation fronts nucleate, denoted z_+ and z_0 in Fig. 6, which shows the evolution of the fronts with the temperature calculated using the material data listed in Tab. 2. In the region between z_+ and z_0, both multi- and single-variant martensite transform into austenite. At the temperature T_1 = 90.4 °C, the fronts z_m and z_+ coalesce, thus for $T>T_1$ multi-variant martensite transforms into austenite between the origin and the front z_0, and single-variant martensite transforms into austenite between $z_+(=-\lambda)$ and z_0. At $T = A_f$, the transformation of both martensite variants into austenite finishes and the beam recovers its original (memorised) curvature χ_0. As the fronts evolve, the curvature of the beam also evolves along the continuous curve plotted in Fig. 7. Correspondingly, the single-variant martensite fraction and stress distributions also change inside the cross-section and Fig. 8 shows the calculated evolutions. The details for calculating the curves shown in Fig. 6, 7 and 8 are given in [20].

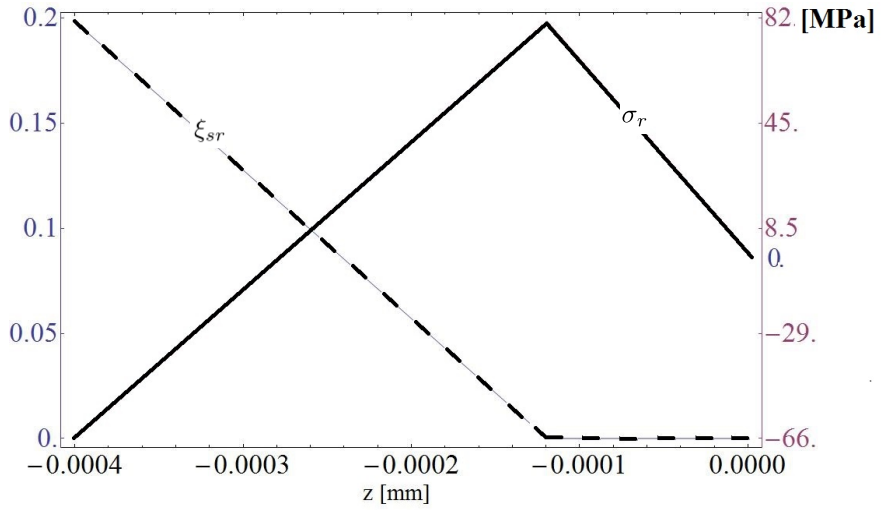

Figure 5: Calculated stress (σ_r) and single-variant martensite (ξ_{sr}) residual distributions after the first bending. For symmetry reasons, only the distributions in the upper half of the cross-section are shown.

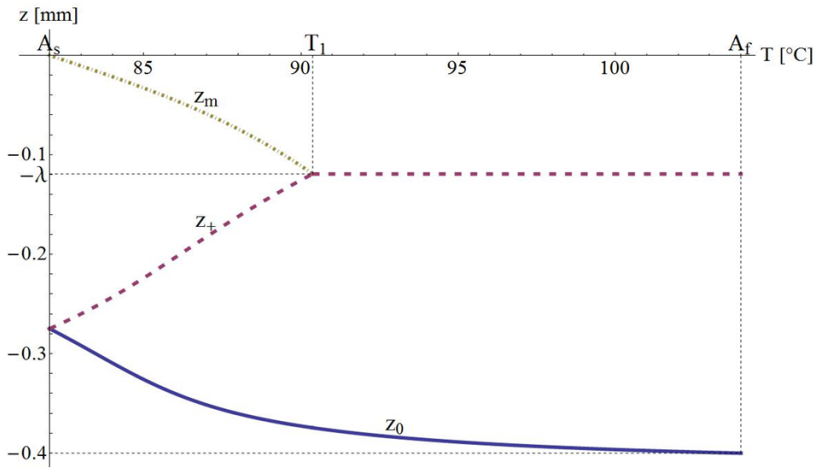

Figure 6: Calculated evolution of the phase transformation fronts with the temperature; z indicates the coordinate along the thickness of the cross-section. At the temperature A_s, single-variant martensite is present only below λ (cfr. Fig. 5) and multi-variant martensite is present throughout the cross-section. For temperatures between A_s and T_1, multi-variant martensite transforms into austenite in the region between the origin and the front z_m (dot-dashed line), and both multi-variant and single-variant martensite transform into austenite in the region between the fronts z_+ (dashed line) and z_0 (continuous line). At the temperature T_1, the fronts z_m and z_+ coalesce, thus for $T>T_1$ multi-variant martensite transforms into austenite between the origin and the front z_0 and single-variant martensite transforms into austenite between $z_+(=-\lambda)$ and z_0.

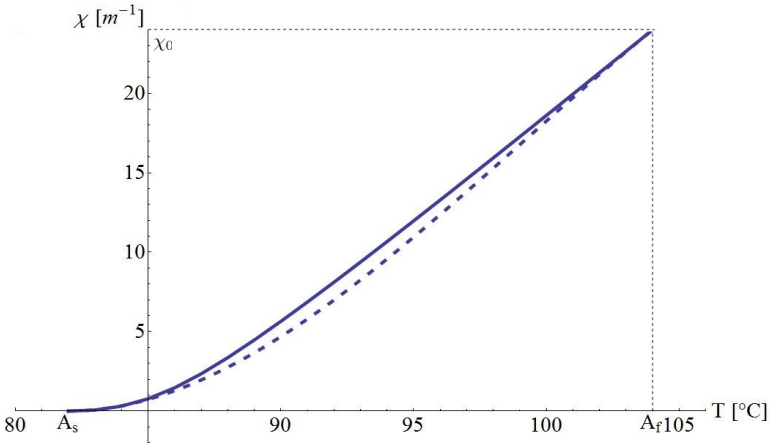

Figure 7: Calculated curvature evolution (continuous line) and its cubic approximation based on Eq. (6) (dashed line) for the first free recovery upon heating.

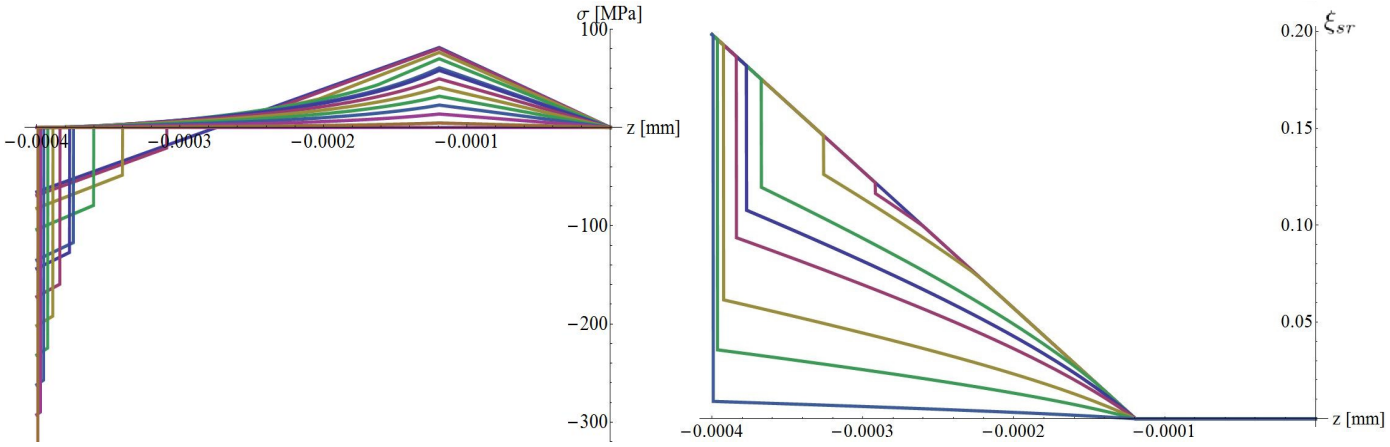

(a) (b)

Figure 8: Calculated evolution of the stress distribution (a) and of the single-variant martensite fraction distribution (b) in the upper-half of the cross-section for the first free recovery upon heating.

The front z−, also described in the solution proposed in [20] and corresponding to the transformation of the martensite in the compressed part of the cross-section, does not exists here because, given the material parameters listed in Tab. 2, it would violates the activation conditions of the kinetic laws. Indeed one has[1]:

$$\frac{C_A\left(A_f - A_s\right)}{E\epsilon_L\xi_{sr}(-h/2)} < \frac{\lambda(\chi_0 - \chi_r)}{\epsilon_L\,\xi_{sr}(-h/2) - (\chi_0 - \chi_r)(h/2 - \lambda)} \tag{5}$$

which implies that the phase transformation occurs only in traction. If condition (5) applies, then the evolution of the front z_0 displayed in Fig. 6 suggests an asymptotic behavior of the function $T \longrightarrow \chi(T)$ near A_f. Indeed, the expression for z_0 (Eq. (40) in [20]) is:

$$z_0(T) = \frac{\xi_{sr}(-h/2)\lambda\, f(T)\epsilon_L}{\left(\chi_0 - \chi(T)\right)\left(h/2 - \lambda\right) - \epsilon_L\, f(T)\xi_{sr}(-h/2)} \tag{6}$$

1 Condition (5) is equivalent to the condition $E_*(z_0) < 0$ (see [20]).

where $f(T)=(A_f-T)/(A_f-A_s)$, and $\xi_{sr}(-h/2)=0.2$ is the value taken by the single-variant martensite distribution at the point $z=-h/2$ at the end of the uniform bending at low temperature ($\xi_{sr}(-h/2)=0.2$ for the parameters listed in Tab. 2, see Fig. 5). Thus, assuming that $z_0 \sim(-h/2)$ as $T \longrightarrow A_f$ and using (6), one obtains the following asymptotic behavior of $\chi(T)$ near A_f:

$$\chi(T) \approx \chi_0 - \frac{2}{h}\epsilon_L \frac{(A_f - T)}{(A_f - A_s)}\xi_{sr}(-h/2) \tag{7}$$

One could tentatively approximate the curvature evolution with a cubic curve having minimum at $T=A_s$ (and the minimum value is χ_r) passing through the point (A_f, χ_0) and having tangent line at $T=A_f$ given by (7). For the material parameters of the alloy studied in this paper, the result turns out to be in acceptable agreement with the exact curvature evolution in almost all the range of temperatures (A_s, A_f), as shown in Fig. 7.

So far only the first free recovery upon heating has been considered, and the results have been obtained under the assumption that the beam recovers completely its original curvature χ_0 at $T=A_f$. However, the experimental data described in the previous sections indicates that this does not occur, and that the curvature recovered at the end of heating decreases with the number of cycles. This could be attributed to the presence of residual martensite in the parent phase at macroscopic free stress state, due to accumulation of plastic dislocations. Experimental evidence of residual strain due to accumulated martensite has been reported in [23, 29].

To phenomenologically describe the accumulation of martensite, one could assume that $\xi_{sr}(-h/2)$ depends upon the number n of cycles as follows:

$$\xi_{sr}(-h/2;n) = (1-e^{(1-n/n_0)})\xi_\infty + \xi_0 \tag{8}$$

where $\xi_0 = 0.2$ is the value calculated for the first cycle, n_0 and ξ_∞ are two material parameters. Substituting (8) into (7) gives an equation for the curvature evolution near A_f with the number of cycles. Fig. 9 shows the plot of the curvature at $T=101$ °C as a function of n obtained with the following values of the material parameters: $n_0 = 4.75$ and $\xi_\infty = 0.32$. These values have been chosen so as to fit the experimental data at high temperature (points labeled with the circles in Fig. 9) as close as possible.

Fig. 9 shows also the numerical results obtained using the model proposed in [25], which is adopted to reproduce the experimental data during the training and in particular, the evolution of the curvature at high temperature during the cycles.

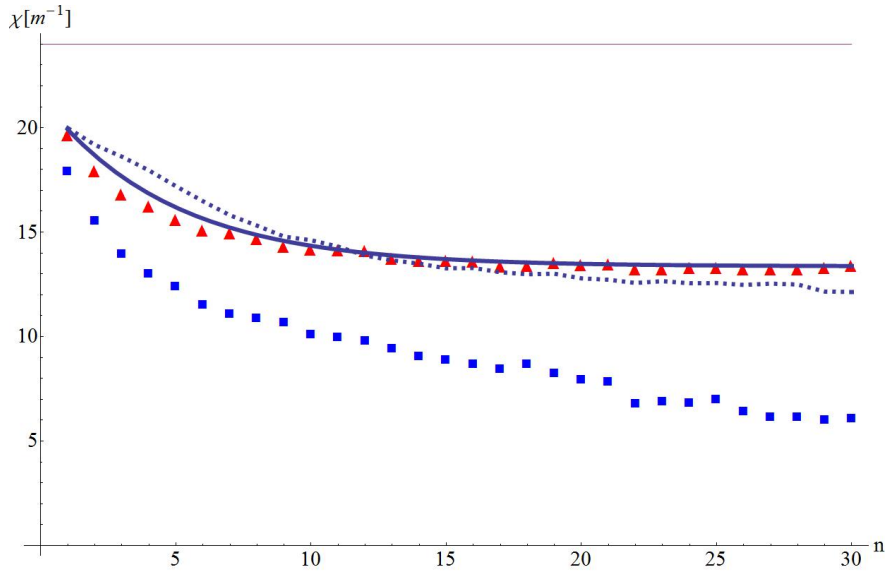

Figure 9: Evolution of the recovered curvature with the number of cycles. Triangles: recovered curvatures measured at high temperature. Squares: recovered curvatures measured at low temperature after cooling. Continuous line: theoretical evolution based upon the phenomenological assumption (8). Dotted line: simulated evolution based on the model proposed in [25].

CONCLUSIONS

The bending behaviour of a NiTi strip, trained in order to induce the TWSME, was experimentally and theoretically investigated. The evolution of the curvature with the increasing number of training cycles revealed that the memory of the cold shape progressively increases. This effect can be attributed to dislocations rearrangements produced during the training process and the resulting accumulation of residual martensite, which has been previously reported in traction tests [23, 29]. Even though the martensite accumulation improves the memory of the cold shape, the presence of permanent strains, which is related to the dislocation structure, is thought to be responsible for the degradation of the memory of the hot shape. A one-dimensional phenomenological model was applied to describe the evolution of single-variant martensite and the residual stress in the cross-section of the strip upon uniform bending: single-variant forms initially at the outer and inner fibers of the cross-section and the transformation spreads inside the beam as the value of the applied couples is further increased [20].
An original approximated relation for the evolution of the curvature with the temperature was also proposed and coupled with a phenomenological description of the martensite accumulation, which was assumed to occur during the training process. The resulting evolution of the hot curvature with the number of cycles was compared with the experimental data for the training cycles and with a numerical simulation based on the model proposed by Auricchio et al. [25]. The compared simulations of the curvature evolution were found to be in good agreement with the experimental data. Future developments will concern the simulation of the whole experimental tests adopting the numerical model proposed in [25].

ACKNOWLEDGMENTS

The financial supports of PRIN 2010-11, project "Advanced mechanical modeling of new materials and technologies for the solution of 2020 European challenges" CUP n. F11J12000210001 are gratefully acknowledged. The authors wish also to thank Fratelli Rosati s.r.l. of Leinì (Torino – Italy) for the financial support in this research.

REFERENCES

[1] Liu, Y., Liu, Y., Van Humbeeck, J., Two-way shape memory effect developed by martensite deformation in NiTi, Acta mater., 47 (1999) 199-209.
[2] Liu, Y., McCormick, P.G., Factor influencing the development of two-way shape memory in NiTi, Acta metall. mater., 38 (1990) 1321-1326.
[3] Lagoudas D.C., Shape memory alloys: modeling and engineering applications, Springer-Verlag, (2008).
[4] Perkins, J., Sponholz, R.O., Stress-induced martensite transformation cycling and two-way shape memory training in Cu-Zn-Al alloys, Metall. Trans. A, 15A (1984) 313-321.
[5] Scherngell, H., Kneissl, A.C., Influence of the microstructure on the stability of the intrinsic two-way shape memory effect, Mater. Sci. Eng. A, 273-275 (1999) 400-403.
[6] Wang, Z.G., Zu, X.T., Feng, X.D., Lin, L.B., Zhu, S., You, L.P., Wang, L.M., Design of TiNi alloy two-way shape memory coil extension spring, Mater. Sci. Eng. A, 345 (2003) 249-254.
[7] Wang, Z.G, Zu, X.T., Dai, J.Y., Fu, P., Feng, X.D., Effect of thermomechanical training temperature on the two-way shape memory effect of NiTi and TiNiCu shape memory alloys springs, Mater. Lett., 57 (2003) 1501-1507.
[8] Lahoz, R., Puértolas, J.A., Training and two-way shape memory in NiTi alloys: influence on thermal parameters, J. Alloys Compd., 381 (2004) 130-136.
[9] Lahoz, R., Gracia-Villa, L., Puértolas, J.A., Training of the two-way shape memory effect by bending in NiTi alloys, J. Eng. Mater. Technol., 124 (2002) 397-401.
[10] Merlin, M., Soffritti, C., Fortini, A., Studio del trattamento termico di lamine in lega a memoria di forma NiTi per la realizzazione di strutture funzionali, La Metallurgia Italiana, 11-12 (2011) 17-21.
[11] Wasilewski, R.J., On the "reversible shape memory effect" in martensitic transformation, Scr. Metall., 9 (1975) 417-421.
[12] Guilemany, J.M., Fernández, J., Effect of training time on two way shape memory effect obtained by stabilised stress induced martensite, Scr. Metall. Mater., 30 (1994) 59-61.

[13] Luo, H.Y., Abel, E.W., A comparison of methods for the training of NiTi two-way shape memory alloy, Smart Mater. Struct., 16 (2007) 2543-2549.
[14] Perkins, J., Hodgson, D., The two way shape memory effect, in: Duerig, T.W. et al (Eds.), Engineering aspect of shape memory alloys, Butterworth-Heinmann, (1990) 195-206.
[15] Kohl, M., Dittmann, D., Quandt, E., Winzek, B., Miyazaki, S., Allen, D. Shape memory microvalves based on thin films or rolled sheets. Mater. Sci. Eng. A 273-275, (1999) 784-788.
[16] Winzek, B., Sterzl, T., Quandt, E. Bistable thin film composites with TiHfNi shape memory alloys. In: Proceedings of the International Conference Transducers '01/Eurosensors XV, vol. 1, pp. 706–709. München, Germany (2001).
[17] Roh, J., Bae, J. Thermomechanical behavior of Ni-Ti shape memory alloy ribbons and their numerical modeling. Mech. Mater. 42, (2010) 757-773.
[18] Irzhak, A., Kalashnikov, V., Koledov, V., Kuchin, D., Lebedev, G., Lega, P., Pikhtin, N., Tarasov, I., Shavrov, V., Shelyakov, A. Giant reversible deformations in a shape-memory composite material. Tech. Phys. Lett. 36, (2010) 329-332.
[19] Meng, X., Cai, W., Zheng, Y., Rao, Y., Zhao, L. Two-way shape memory effect induced by martensite deformation and stabilization of martensite in Ti36Ni49Hf15 high temperature shape memory alloy. Mater. Lett. 57, (2003) 4206–4211.
[20] Rizzoni, R., Merlin, M., Casari D., Shape recovery behaviour of shape memory thin strips in cylindrical bending: experiments and modelling, Continuum Mech. Therm., 25 (2013) 207-227.
[21] Kirindi, T., Sari, U., Dikici, M. The effects of pre-strain, recovery temperature, and bending deformation on shape memory effect in an Fe–Mn–Si–Cr–Ni alloy. J. Alloy. Compd. 475, (2009) 145-150.
[22] Balak, Z., Abbasi, S. M., Effect of primary microstructures during training producers on TWSME in NiTi alloys. Int. J. Eng., 25, (2012), 337-341.
[23] Saint-Sulpice, L., Arbab Chirani S., Calloch S., A 3D super-elastic model for shape memory alloys taking into account progressive strain under cyclic loadings. Mech. Mat., 41 (2009) 12-26.
[24] Mehrabi, K., Bruncko, M., Kneissl, A. C., Microstructure, mechanical and functional properties of NiTi-based shape memory ribbons. J. Alloys Compd., 526 (2012) 45-52.
[25] Auricchio, F., Marfia, S., Sacco, E., Modelling of SMA materials: training and two-way memory effects, Comput. Struct., 81(2003) 2301-2317.
[26] Khandelwal, A., Buravalla, V., Models for shape memory alloy behavior: an overview of modeling approaches, Int. J. Struct. Changes Solids Mech. Appl., 1 (2009) 1-30.
[27] Paiva, A., Savi, M.A., An overview of constitutive models for shape memory alloys, Math. Prob. Eng., (2006) 1-30.
[28] Marfia, S., Rizzoni, R., One-dimensional constitutive SMA model with two martensite variants: Analytical and numerical solutions, Eur. J. Mech. A. Solids, 40 (2013), 166-185.
[29] Kang G., Kan Q., Qian L., Liu Y., Ratchetting deformation of super-elastic and shape-memory NiTi alloys, Mech. Mat., 41 (2009) 139-153.